Surrounding Size effect on Brightness Contrast-to-Assimilation is Predicted in Retina

Jihyun Kim
and
Marcelo Bertalmío

Departament de Tecnologies de la Informació i les Comunicacions
Universitat Pompeu Fabra
Carrer del Roc Boronat 138
08018 Barcelona
Spain
Contact: jiboon.kim@gmail.com

Abstract

Brightness (perceived luminance) of a target area in a visual scene depends on luminance of the surfaces surrounding this area (brightness induction). The quantity and quality of the induction are further altered by the size of the surrounding surfaces such that a large surrounding surface induces strong contrast onto the target area but a small surface induces weak contrast or assimilation. While contrast induction is attributed to a local-range lateral inhibition in the retina, there is little consensus on a neural structure underlying assimilation. Some studies postulated that assimilation occurs by an unknown post-retinal mechanism that performs long-range surface interaction. However, we propose that such long-range mechanism exists in the retina based on recent neurophysiological evidence that the main retinal inhibitory feedback interneurons manifest wide receptive-fields (RFs). We cross-examined the effect of these wide RFs in two different biophysical retinal model platforms (van Hateren, 2005; 2007; Wilson, 1997) and confirmed that the cell responses in both of the models match to behavioral data of the brightness contrast and assimilation as a function of surrounding surface size (Helson, 1963; Reid & Shapley, 1988), if and only if the wide RFs are considered. To the best of the authors' knowledge, this is the first evidence that the wide RFs of inhibitory interneurons serve for long-range surface interaction, that local contrast and long-range surface interaction share the same neural locus, and that brightness assimilation is inaugurated at the retinal level.

Keywords: Spatial induction, Brightness, Assimilation, Contrast, Retinal processing

Introduction

Despite the long history and volume of the behavioral investigation on brightness induction phenomena, there is no clear accordance between brightness computation theories and neural structures that accomplish such computation (Kingdom, 2011). One of the challenges comes from the observation that the direction of brightness induction changes depending on the size of the surrounding surface: decreasing the spatial extent of the surrounding surface decreases brightness contrast (target brightness pushed away from the surrounding luminance) and rather induces assimilation (target brightness pulled toward the surrounding luminance) beyond some point of the decrement (Helson, 1963; Reid & Shapley, 1988; Rudd, 2010). Let us note that in some literature 'lightness induction' is used instead of 'brightness induction', and in some works the size effect is more generally addressed as the ‘spatial frequency’ dependency of spatial induction.

An example of such bi-directionality of spatial induction was demonstrated by Helson (1963; refer to Figure 4a in the section **Experiment 1**). Using a stimulus comprised of a set of white bars (the left half of stimulus) and a set of black bars (the right half of stimulus) that were drawn on the homogeneous grey surface, Helson investigated the brightness induction by white v.s. black bars onto the grey area when bar widths were varied. The results showed that the brightness of the grey area among the white bars appeared darker compared to that among black bars when the white and the black bars were sufficiently wide (brightness contrast). However, reducing the width of the bars decreased the strength of spatial contrast effect, and with very thin bars, the grey area among white bars was perceived to be lighter than that among the back bars (brightness assimilation). These results suggest that decreasing the spatial scale of the white and the black bars gradually changed the direction of brightness induction from contrast to assimilation.

Another evidence of the surrounding-size-dependent brightness contrast-to-assimilation was reported by Reid and Shapley (1988; refer to Figure 5a in the section **Experiment 2**). In this study, Reid and Shapley introduced a mechanical interpretation to the concepts of contrast and assimilation and verified their claims in behavioral experiments. In specific, Reid and Shapley defined contrast as the antagonistic luminance processing between a pair of bordering surfaces (local contrast effect). Assimilation was defined as the effect that counteracts to the local contrast effect and was proposed to result from the contribution of non-bordering surfaces on brightness computation via a sort of long-distance surface interaction (Arend, Buehler, & Lockhead, 1971; Fry and Alpern, 1953; Heinemann & Chase, 1994; Shapley & Reid, 1985). Based on these definitions, the authors argued that a large

surrounding surface induces strong brightness contrast that overrides any contribution of assimilation, while assimilation is observed when the spatial scale of the surrounding is too small to induce any significant contrast.

To test this idea, Reid and Shapley (1988) presented two identical disk-and-ring stimuli (the same physical contrast between the disk and the ring), one on a dark and the other on a light background field, and compared the brightness of the disks in the two stimuli. This method allowed to exclusively quantify the magnitude of assimilation (the influence of background onto the disk brightness through long-range interaction) induced by different widths of rings while the amount of brightness contrast (brightness induction by the ring to the disk by local contrast) was fixed. The results showed that the brightness of the disk in the dark background appeared lighter than the one in the light background (assimilation) but the magnitude of this assimilation (difference of the brightness between the two disks) gradually increased as a function of decreasing ring width, supporting that decreasing the surrounding surface size decreases contrast and increases assimilation.

Between the two mechanisms that interactively regulate brightness induction in Reid and Shapley's (1988) argument, the neural mechanism for local contrast was attributed to the lateral inhibition in the retina (see also Heinemann & Chase, 1994; Ratliff, 1971; Shapley & Enroth-Cugell, 1984). This attribution is consistently reinforced by neurophysiological evidence asserting that the lateral inhibition in the visual system is accomplished through the center-surround spatial antagonism in the retinal feedforward cells and inhibitory feedback interneurons as illustrated in Figure 1 (Lee, Martin, & Grünert, 2010; Perlman & Normann, 1998; Thoreson & Mangel, 2012). However, a coherent theory on the underlying neural mechanism of assimilation (or long-range surface interaction mechanism) is absent (Fiorentini, 2003; Reid & Shapley, 1988; Rudd, 2010). Reid and Shapley along with other researchers (Heinemann & Chase, 1994; Rudd, 2010) suggested that assimilation is allegedly post-retinal given that the range of spatial extent that generates a distinguishable assimilation effect (~1°) much exceeded the center-surround RF size reported in singe cell recording studies on ganglion cells.

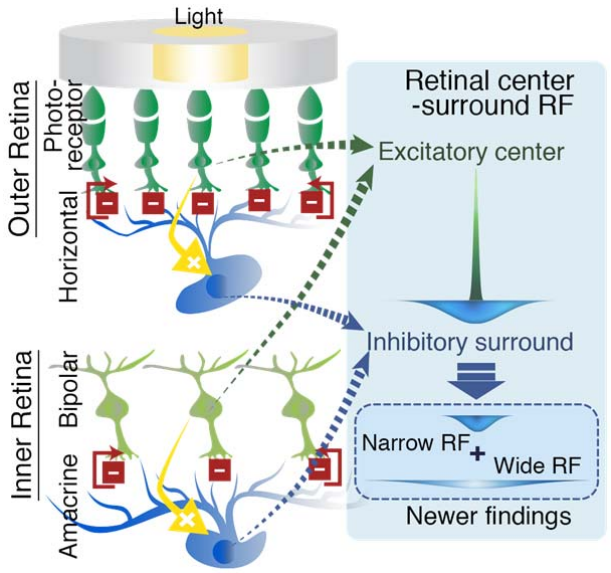

Figure 1. Lateral inhibition process in the retina and formation of the center-surround RF. Lateral inhibition in the retina occurs as the feedback from interneurons (horizontal cells and amacrine cells), which receive excitatory inputs from photoreceptors and bipolar cells, respectively, inhibits the excited photoreceptors and bipolar cells, as well as the neighbors of the excited cells due to the interneurons' spatially converging RF. The typical center-surround RF structure in the retinal ganglion cell is a product of interneurons with larger RFs creating inhibitory surround around the excitatory center of the smaller-RF feedforward cells. The current study tests the effect of wide RF profile of these interneurons, in addition to the conventional (narrow) RF structure, based on the newer neurophysiological evidence (inset).

The current study, however, reports evidence against the claim that assimilation should occur post-retinally. We found that the post-retinal assumption is contradicted by taking into account for newer neurophysiological discoveries on spatially extended RF profiles (wide RF; > 500-1000 μm) of horizontal cells and some types of amacrine cells in addition to their classic local scale RF profiles (narrow RF; < 100-300 μm; the surround RF conventionally measured in ganglion cells; see Figure 1, inset; Kolb, 1997; Lin & Masland, 2006; MacNeil & Masland, 1998; Packer & Dacey, 2002; 2005; see also Kaplan & Benardete, 2001; Passaglia, Enroth-Cugell, & Troy, 2001; Solomon, Lee, & Sun, 2006). The role of narrow RFs of retinal interneurons has been broadly discussed regarding how they form the surround field of the ganglion cell RF and regulate the ganglion cell's gain control properties (Benardete & Kaplan, 1999a; Benardete & Kaplan, 1999b; Kaplan & Benardete, 2001; Thoreson & Mangel, 2012; Wilson, 1997), contrary to that the functional contribution of

wide RF components to retinal spatial processing has not been discussed. We computationally evaluated the effect of the wide RFs in two realistic biophysical retinal models built solely on the neurophysiological premises (Figure 2; van Hateren, 2005; 2007; Wilson, 1997) and discovered their functional contribution to long-range surface interaction.

We made an effort to make our simulation as conclusive as possible in the following manner. The two biophysical retinal models used in this study allow virtual simulations of the voltage responses of cells in a realistic retina (Figure 2; van Hateren, 2005; 2007; Wilson, 1997). Both of the models take in inputs as realistic 2-D images identical to those in the behavioral studies in projected retinal sizes and troland intensities. Using these models, we designed the simulation methods as the intuitive and straightforward parallels to the behavioral experiments. Also, we used a single fixed parameter set for the entire simulation to avoid the complication of data fitting so as to make a forthright comparison of the simulation results between the two models and to demonstrate the computational robustness of our claim (see the section **The Retinal Models** below for details).

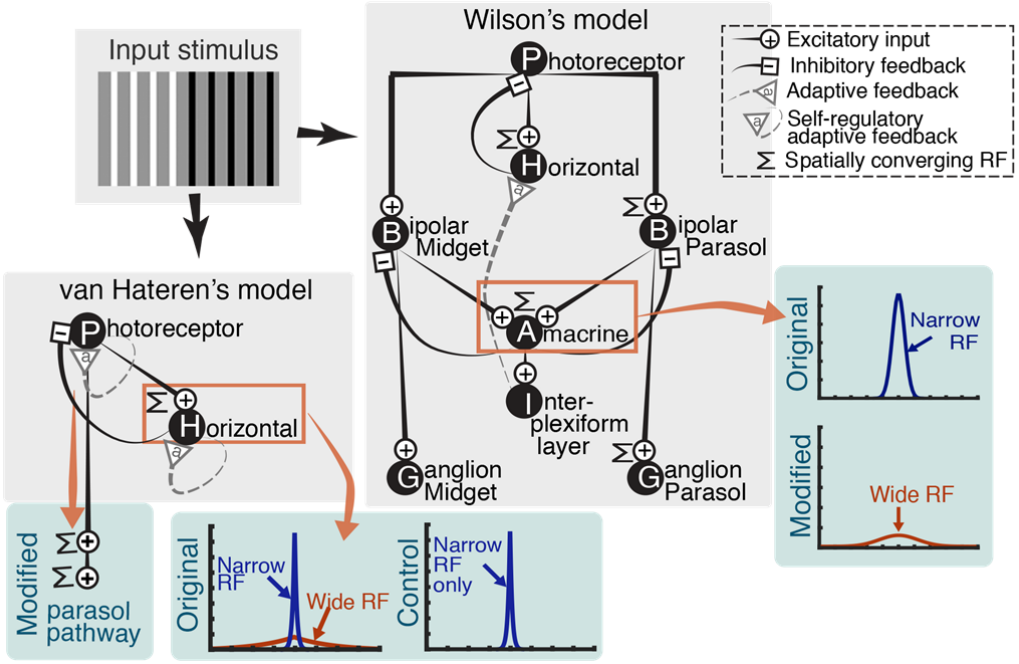

Figure 2. Diagrams of the algorithmic structures of the two retinal models by Wilson (1997) and van Hateren (2005; 2007) and the modifications made to the models in the current study. Inside the grey box shows the original versions of the models, and the modifications made in the current study are shown in green boxes led by the red arrows. See the text for more details.

To account for Helson's (1963) contrast-to-assimilation phenomenon by bar width, we needed to make structural modifications to both of the models (adding wide RF to Wilson's model and adding a parasol pathway structure to van Hateren's model as illustrated in Figure 2; these modifications were as minimal as possible to preserve the capacity of the original models in predicting neurophysiological and/or behavioral data; see the following sections for details). After these modifications, both of the model responses matched to the pattern of the behavioral data from Helson's experiment. Reid and Shapley's (1988) data were readily explained in van Hateren's model, and Wilson's model could predict the result when the wide RF of the interneuron was added to the original model structure. These results altogether showed that wide RFs of interneurons produce the systematic effect of surrounding size in the contrast-to-assimilation phenomena reported by Helson and Reid and Shapley.

The Retinal Models

Each of the retinal models by Wilson (1997) and van Hateren (2005; 2007) has different advantages in terms biological plausibility. The model by Wilson contains a comprehensive retinal structure embodying all the main layers and parallel processing pathways but this model computes the cell responses in a mathematically abridged way (less quantitative precision to neurophysiological data fit). The model by van Hateren embodies only the photoreceptor and the horizontal cell layers while the model realizes complicated algorithmic process for the internal dynamics of each class of the cells, the responses of which quantitatively match to a large collection of neurophysiological data. Taking advantage of the fact that the algorithmic structures are markedly different between the two models, we intended to identify robust mechanical features by which both of the models predict the brightness data patterns, regardless of the algorithmic details of each model.

To make the model simulations straightforward for this goal, we imposed some basic principles. First, all the model parameters were fixed throughout the simulations to the values used in the original studies except for the variables systematically investigated. All the simulation conditions of interest (i.e. with or without wide RF and with or without parasol pathway spatial processing) were tested in the identical setting described in the following sections, with the only manipulation to the models being the change of RF size or presence / absence of a certain filter structure. Second, the simulation methods were identical to those of the original behavioral studies (Helson, 1963; Reid & Shapley, 1988). In fact, one of the reasons of choosing Wilson's and van Hateren's models over other available retinal models (Hennig, Funke, & Wörgötter, 2002; Shah & Levine, 1996; Wohrer & Kornprobst, 2009) was that these two models realize light adaptation process that follows behavioral (Wilson's

model) or neurophysiological (van Hateren's model) data under varying background illumination. The light adaptation feature enables the models to take in the input stimulus comprised of values in luminance units (in troland) rather than in normalized scales (e.g. 0-1 or 0-255) and with the background illumination values designated such that the experimental methods of the behavioral studies could be directly applied to the model simulations.

We first concisely introduce the retinal models by Wilson and by van Hateren and make notes on our implementation details while referring to the original studies for most of the details of the model algorithms.

The Model by Wilson (1997)

The retinal model by Wilson (1997) is developed to demonstrate the functional architecture of the retinal circuitry (Figure 2, Wilson's model). The model embodies a full set of basic anatomical layers that are comprised of photoreceptors (cones without considering spectral sensitivity), horizontal cells, parasol and midget ON and OFF bipolar cells, ON and OFF amacrine cells, interplexiform layer cells, and parasol and midget ON and OFF ganglion cells. Functionally, photoreceptor and horizontal cell layers pair to form a local feedback circuit and, similarly, parasol/midget ON (OFF) bipolar and ON (OFF) amacrine cell layers are paired. Interplexiform layer cells receive inputs from amacrine cells and send inhibitory signals back to horizontal cells thereby forming a long-range feedback circuit that adaptively adjusts the gain and speed of horizontal cell responses. These local and long-range interneuron feedbacks gate the feedfoward signals transmitted along photoreceptors, bipolar cells and ganglion cells and accomplish light adaptation and contrast gain control. The center-surround spatial processing structure observed in the ganglion cell RF is formed by the dynamic interactions among feedforward cells and feedback interneurons.

In the original model, the spatial extents of the inhibitory surround, i.e. the inhibitory interneuron RF sizes, are within the narrow- to small-field range (Kolb, 1997) in Wilson's model (RF defined as a 2-dimensional Gaussian unit point-spread function, e^{-r^2/σ^2}, where r is the distance from the RF center and σ is the spatial constant in visual angle; the spatial constant for the horizontal cells is 0.08°, and that for amacrine cells is 0.15°). As to the formation of the excitatory center, the parasol pathway signals are spatially converged at the bipolar cell (averaging three neighboring photoreceptor inputs) and at the ganglion cell (spatial constant 0.033°) feedfoward synapses. In the midget pathway, signals are not spatially converged (one-to-one synaptic correspondence along the feedforward layers).

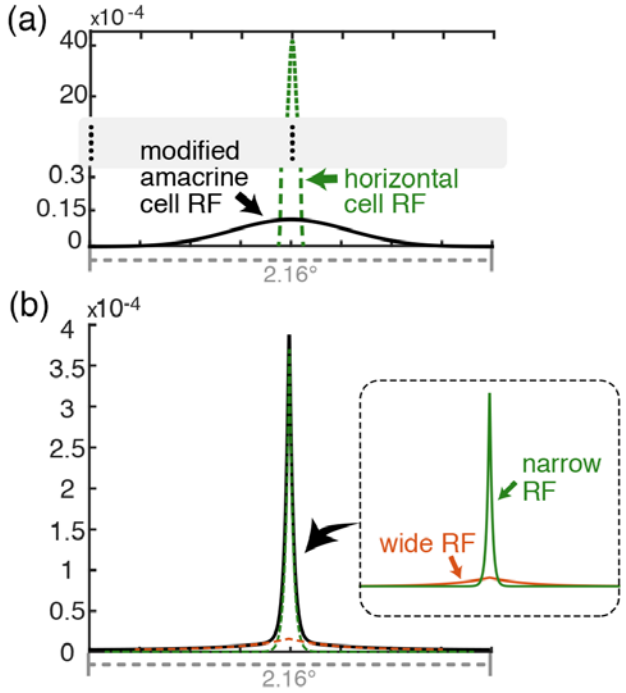

Figure 3. The realistic scale illustration of the filters for wide RFs. (a) The coronal plot of the 2-dimensional amacrine cell wide-RF filter profile (solid black line) that was modified in the current study from the original study (Wilson, 1997). The dotted green line shows the horizontal cell filter profile (narrow RF) in the same scale for comparison. (b) The horizontal cell narrow + wide RF filter in van Hateren's model (2005; 2007). The solid black line illustrates the actual filter profile and the dotted lines in the plot and the solid lines of the corresponding colors in the inset separately shows the narrow (green) and wide (red) components that comprise the filter for comparison. Note that the weights of the wide RF of both of the filters are much smaller than that of narrow RF.

Introducing the wide-RF interneuron feedback by changing the amacrine cell RF was the only modification made to Wilson's model in the current study compared to the original study. To make the direct comparison of the effect of the wide RF by this modification to the results of van Hateren's model, this RF size was set to roughly correspond to the size of the wide horizontal cell RF in van Hateren's model (spatial constant 1.47°). The RF profile used in the simulation is plotted in Figure 3a (solid black line) together with the horizontal cell RF (dashed green line) in the same scale for comparison. In reality, the types of different amacrine cells are abundant, with many of them anatomically classified as wide-field cells (dendritic field diameter > 500 μm). However, the functional roles and precise synaptic connectivity structures of varying types of amacrine cells are subject to future studies and

how far and which type of these cells could shape the retinal spatial processing as we demonstrate through the model, if they do, is an open question.

It should also be noted that, in the original study by Wilson (1997), all the simulations were performed in 1-dimensional space merely to reduce computation time while the model algorithms were readily extendable for 2-dimensional simulations. We did extend Wilson's model for 2-dimensional simulations in the current study. Note that this extension slightly changes Equation (4) of the original article (a bipolar cell averages three neighboring photoreceptors' inputs in the 1-dimensional simulations in Wilson, 1997, but this changes to averaging 3x3 neighboring photoreceptors in the 2-dimensional simulation).

The Model by van Hateren (2005; 2007)

van Hateren (2005; 2007) developed a state of the art partial retinal circuitry model that implements a cascade of phototransduction process in photoreceptors (see also van Hateren & Lamb, 2006) and the inhibitory feedback from the horizontal cells to photoreceptors. As in Wilson's model, the spectral sensitivity of different photoreceptor types is not considered.

The initial version of the model (van Hateren, 2005) only dealt with temporal dynamics of the photoreceptor-horizontal cell circuitry. Later van Hateren (2007) improved the functionality of the model's horizontal cells by adding spatial processing features (i.e. RF structures) as well as the light-adaptive horizontal cell response gain and time course changes (refer to Figure 1C in van Hateren, 2007). The two versions of the model slightly differ in terms of the mathematical details, and here we reference to the algorithms described in the latter version (van Hateren, 2007).

The feedback signals from horizontal cells to photoreceptors generate inhibitory surround of the center-surround spatial processing. The horizontal cell RF structure in van Hateren's model is directly taken from neurophysiological studies (Packer & Dacey, 2001; 2005), which showed that the RF of a horizontal cell exhibits a dual-component profile that is well represented as a weighted sum of two exponential unit point-spread functions ($e^{-r/\lambda}$; r is the distance from the RF center; λ is a spatial constant in μm; for more details about the RF structure, see the section **A two-component spatial receptive field** in van Hateren, 2007), one exponential function with the small spatial constant (narrow RF component) and the other with the large spatial constant (wide RF component) as illustrated in Figure 3b. The narrow RF component results from the direct dendritic connection from photoreceptors to horizontal cells, while the wide RF component results from electric coupling among adjoining horizontal cells. In the original study of van Hateren, the suggested generic

parameter values for these spatial constants were 20 μm in radius for narrow RF component and 300 μm for wide RF component. We conformed to these values in the current study. While the RF in the original study was applied by autoregressive-moving-average filtering to the input in the hexagonal direction, we simplified the computational process by generating a 2-dimensional filter in the shape of the given dual-component RF and performing the filtering in the frequency domain.

For the control simulations in which we tested the effect of narrow RF only (in the sections **Experiment 1** and **Experiment 2**) and wide RF only (in the section **Simulation without Narrow RF**), we simply generated the filters with a single exponential function, only with the smaller spatial constant for the former and only with the larger spatial constant for the latter.

Since van Hateren modeled only partial retinal circuitry, an additional assumption was needed to test the effect of the spatial convergence of the parasol pathway. As a minimal treatment for this purpose, we passed the model photoreceptor responses through two stages of spatial convolution with each stage representing the RF of diffuse bipolar cells and of parasol ganglion cells. We defined the corresponding RF structures (i.e. spatial filter shapes) to be identical to those used in Wilson's model (1997; a 3 x 3 grid averaging filter for bipolar cell and a Gaussian filter with the standard deviation of 0.033° for ganglion cell).

For computational convenience, we omitted one minor temporal adaptation feature that was introduced in the later version of the model (adaptive temporal filtering feature, see Figure 1C in van Hateren, 2007). As pointed out by van Hateren (page 8, in the section **Adaptive temporal filtering** in van Hateren, 2007), this feature was implemented for a slightly better quantitative fit of model responses for high temporal-frequency stimulations (80 Hz) of a large stimulus with a homogeneous surface (10°). However, since the improvement of data fit by this feature was relatively unremarkable and such temporal precision at high temporal frequency range is irrelevant in the context of the current study, we bypassed this feature. All the rest of the model algorithms were intact from the original study and the parameters were fixed throughout the simulations to the generic values proposed by the author (Table 1 in van Hateren, 2007).

General Simulation Methods

Retinal Projection

The visual field (i.e. the retinal area on which the stimulus was projected) was restricted to 8° for all model simulations. The stimuli were projected at the center of this projection area

in sizes as specified in the behavioral studies. The initial values of the cells in each retinal layer were set to resting potential values (or, in an algorithmic term, steady state values of the equations) to the adapting light intensity (i.e. uniform illumination over the entire visual field) in each experiment.

We applied foveal photoreceptor density uniformly for the entire visual field (i.e. projection area) and disregarded the radial density reduction as a function of retinal eccentricity (fovea v.s. periphery). The foveal cell density was set to 146000 *photoreceptors/mm*^{2} (111 x 111 cells per square degree) following Wilson's model (1997).

While our assumption on the cell density needs to be interpreted with a caution, we considered that disregarding the change of the spatial sampling rate across the retinal surface is rather compatible to the fact that, in reality, observers in the behavioral experiments (Helson, 1963; Reid & Shapley, 1988) were not restricted from eye movements, in which case the observers would move their eyes to refocus different areas of the stimulus onto the fovea. This assumption on cell density is relatively unimportant for the simulations of Reid and Shapley's experiment in which the maximum size of the stimuli was 1.8º.

Luminance Unit

Both of the original models by Wilson (1997) and by van Hateren (2005; 2007) are designed to take in troland (retinal illuminance) values. If the behavioral studies provided luminance values in *cd/m*^{2} for stimulus intensity, the provided values were converted into troland unit. As a standard, we set the pupil diameter to 3 mm, which is the value used in Wilson's model. Wilson defined the point-spread function of light scatter corresponding to the 3mm pupil based on Campbell and Gubisch (1966) and we kept all these aspects intact for all the simulations using Wilson's model.

We tested an additional pupil size with van Hateren's model (6.5 mm, from monocular viewing of 8 *cd/m*^{2} field by 30 year old person based on the study by Watson and Yellott, 2012) and confirmed that the results in this study are unaffected by the assumption on pupil size. Noting that assuming a larger pupil size yields bigger troland values in retinal inputs than a smaller pupil size for the same luminance values in *cd/m*^{2}, this means that our results are robust over different retinal illumination range.

Data Acquisition

Since the retinal models compute voltage responses that change across time, it is rather arbitrary to set a particular point in time in which the cell responses correspond to a perceptual experience. Given the difficulty, we have chosen the time point for data acquisition to be at 300 ms after stimulus onset (assuming that a stimulus did not set off

before 300 ms). This time scale allows all the short-term feedback effect (i.e. the inhibitory feedback from horizontal and amacrine cells in Wilson's model, 1997; immediate feedback from horizontal cell without the effect of adaptive gain in van Hateren's model, 2007) to be stabilized, while this duration is insufficient for the long-term adaptive system to take significant effect (i.e. interplexiform layer cell feedback to horizontal cells for gain and temporal change in Wilson's model; adaptive horizontal gain change in van Hateren's model). Thus, all the data reported in the current study are derived by analyzing the model cell responses at 300 ms after the stimulus onset.

Temporal and Spatial Filtering

For all simulations, the solution of a first-order ordinary differential equation (ODE) for temporal low-pass filtering was approximated by the modified Tustin method (van Hateren, 2008), which is shown to outperform other ODE approximation schemes in terms of computational accuracy and speed among autoregressive moving-average filtering methods. The time step of the temporal evolution was set to 0.1 ms.

The spatial filtering was performed by frequency-domain convolution. As explained in the previous sections (The Model by Wilson and The Model by van Hateren), the spatial filters were generated in the functional forms described in each of the original papers (Gaussian point-spread function in Wilson's model, 1997; weighted sum of a wide and a narrow exponential point-spread functions in van Hateren's model, 2007).

Experiment 1: Bright Induction by Different Widths of Bars (Helson, 1963)

We first focused on identifying the retinal architecture underlying the classic bright contrast-to-assimilation phenomena induced by different width of bars reported by Helson (Figure 4a; 'the second study with Joy' in Helson, 1963). Helson conducted a behavioral study in which sets of black and white bars of varying width (bar width: 0.06°, 0.19°, 0.38°, 0.54°, 0.76°, 0.96°) were drawn on a homogeneous 3.4° x 5.33° rectangular grey field of 36% reflectance and the induction by the bars onto the grey area was measured. The grey area width (i.e. distance between two neighboring bars) was also manipulated (grey width: 0.06°, 0.19°, 0.38°, 0.54°, 0.76°, 0.96°; note that all the different notations of units in the original behavioral studies are converted into coherent units of stimulus size in visual angle degree and stimulus intensity in cd/m^2 throughout the text). The induction effect was measured by rating how much darker (lighter) the grey appears among white bars compared to that among black bars, with higher (lower) score indicating more contrast (assimilation). Figure 4b shows this score as a function of grey area width for different bar widths (a rescaled replot of FIG 2 in Helson, 1963). Demonstrating the bar width effect, a wider bar induced stronger contrast

but the strength of the contrast was reduced and ultimately reversed to assimilation as the bar width decreased.

Model Simulation Method and Results

The stimuli for the model simulations were generated in identical sizes (scaled to retinal-projection sizes) as in Helson's study (1963). Since the absolute luminance values for black and white bars and grey area were not provided in the original study and only the reflectance of the grey area was reported, we set the input stimuli intensity by first choosing the mean luminance intensity, which is assumed to be the mean display luminance (i.e. adapting light intensity; we arbitrarily set this value to 30 cd/m^2), and assuming this value to be the mean luminance level that corresponds to the 50% reflectance grey point (other mean luminance values were tested and confirmed not to affect the results). Then values for the black and the white bars were set to yield Michelson contrast of 90% around this mean luminance level such that the black bars have reflectance of 5% (3 cd/m^2) and white bars 95% (57 cd/m^2) with the homogeneous-illumination assumption. The luminance of the grey region between the black and white bars was set to 36% (22 cd/m^2) as was used by Helson.

The simulation procedure was straightforward. The 36 stimulus conditions (6 bar width x 6 grey width) were simulated and the mean activities of the model cells whose RF fall on the grey stimulus area were computed for each condition. Brightness induction was scored by subtracting the mean voltage of the cells responding to the grey area among white bars subtracted from the mean at grey among black bars (ΔV; positive / negative values indicate contrast / assimilation).

For Wilson's model, we analyzed parasol ganglion cell responses as a standard, for these cells are known to code luminance information (Lee, Pokorny, Smith, Martin, & Valberg, 1990; Lee, Sun, & Valberg, 2011). On the other hand, since van Hateren's model only contains photoreceptors and horizontal cells, we first analyzed the photoreceptor responses as the original model output. Then we imitated a parasol pathway spatial processing structure by passing photoreceptor responses through a two-stage spatial low-pass filter (Gaussian filter with spatial constants equal to the parasol bipolar and ganglion cell RFs used in Wilson’s model).

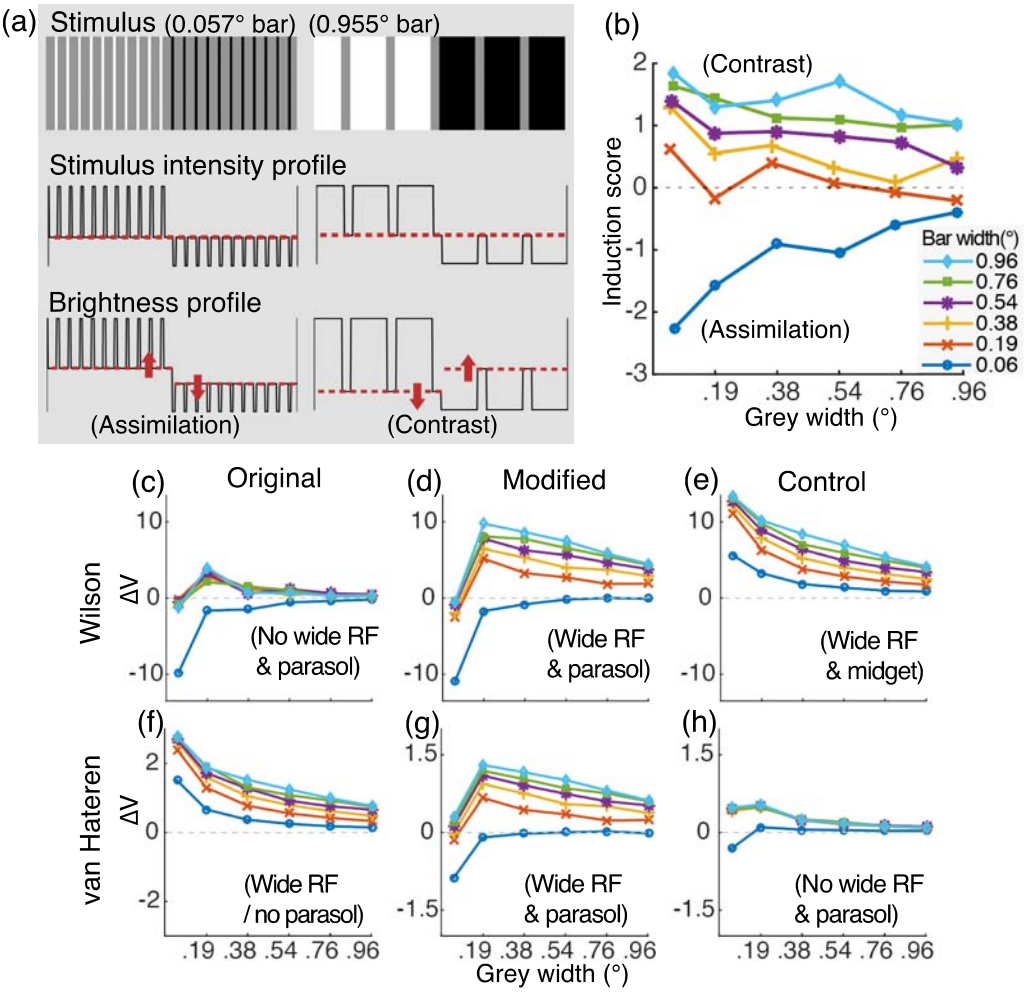

Figure 4. Behavioral and simulation results of Helson's experiment (1963). (a) Examples of stimuli with narrow bars (left) and wide bars (right). The comparison of stimulus intensity profile with brightness profile schematically illustrates how brightness assimilation and contrast are induced, given narrow bars and wide bars, respectively. (b) The behavioral data on the induction direction and strength as a function of grey width for different sizes of bars (replotted from FIG 2 in Helson, 1963). A negative / positive induction score indicates assimilation / contrast. (c-h) The retinal model simulation results. (c-e) for Wilson's model (1997) and (f-g) for van Hateren's model (2005; 2007), with the original algorithms (c, f), modified versions (d, g) and control versions (e, h). All are plotted comparably to (b) except that y-axis is ΔV (mean responses to grey among white bars – grey among black bars). Wide RF + parasol spatial processing structures are necessary to predict the bright contrast-to-assimilation induction with decreasing bar widths comparable to (b).

Simulation results of the two models in their original algorithms showed that the response patterns are different between the models and neither of the patterns matched to Helson's data. The parasol ganglion cell response pattern from Wilson's model did not match to the bar size effect found in Helson's result, except for the narrowest bar (0.06°) that induced assimilation (Figure 4c). On the other hand, photoreceptor responses of van Hateren's model did show distinguishable size effect among different bar widths, but it did not produce assimilation for the narrowest bar (Figure 4f).

When Wilson's model was modified to include a wide-RF of the interneuron, on the contrary, Wilson's model produced bar width effect comparable to Helson's data (Figure 4d). Likewise, parasol cell responses of van Hateren's model showed an equivalent pattern of bar width effect when the spatial convergence structure was introduced (Figure 4g). These results suggest that the wide RFs of the interneurons was necessary to produce the systematic effect of the bar width on brightness contrast-to-assimilation phenomena. We verified this point again by simulating the same experiment when the wide RF component in van Hateren's model was eliminated (parasol cell responses; Figure 4h), which removed the systematic bar width effect.

On the other hand, assimilation by the narrowest bar (0.06°) required parasol pathway spatial convergence. The midget ganglion cell responses in Wilson's model (Figure 4e) showed the same response pattern as the photoreceptors of van Hateren's model (Figure 4f). It should be noted that the wide RF was not imperative for this assimilation, although sufficient in that the assimilation by the narrowest bar could be induced just with the narrow RF alone as well as just with the wide RF alone (see the section **Simulation without Narrow RF** and **Discussion**).

Experiment 2: Ring-size effect in Disk-and-Ring Stimulus (Reid & Shapley, 1988)

We then tested the role of the wide RFs of interneurons regarding ring width effect in a disk-and-ring display observed by Reid and Shapley (Figure 5a). This experiment measured the magnitude of assimilation (the influence of background onto the disk brightness through long-range interaction) by varying ring widths (0°, 0.08°, 0.2°, 0.35°, 0.53°, or 0.71°) while the amount of brightness contrast (brightness induction by the ring to the disk by local contrast) was constant by presenting two disk-and-ring stimuli of identical luminance composition (the disk luminance was 78 cd/m^2 and the ring luminance and the mean display luminance were 70 cd/m^2), one on a dark and the other on a light background field. Observers adjusted the luminance of the disk in the lighter background (D_{B_light}) to match the disk brightness in the darker background (D_{B_dark}). The difference of background luminance was

systematically manipulated ([70, 70] [65, 74], [61, 78], [57, 82], and [53, 86] *cd/m*^{2} with [70, 70], i.e. the same background luminance for both background fields, as the baseline condition in which assimilation strength = 0). As in Figure 5b (replotted and reindexed from Fig. 3 in Reid and Shapley, 1988), the luminance of the matched disk (D_{B_light}) increased as a function of increasing luminance difference of the background fields for each ring width. For wider rings, however, the background effect was smaller (lower slope) than the narrower rings; thus, the narrower the ring is, the stronger the assimilation.

Simulation Method and Results

The input stimuli to the model simulations were entirely identical to the behavioral study. For the analysis of the model outputs, the mean voltage of model cells responding to the disk was set as the indicator of the disk brightness and the luminance of D_{B_light} such that the mean voltage at D_{B_light} equals to the mean at D_{B_dark} was determined (ΔV; larger values indicate stronger assimilation).

The simulation procedure was slightly modified from the procedure of behavioral measure to be suitable for a simulation environment. In the behavioral experiment, observers were presented with the target and the match stimuli sets simultaneously and they continuously compared the appearance of the match disk (adjusted) with the target disk (fixed). For the model simulations, this adjustment process was imitated by performing simulations for the a large match disk luminance range for the match stimulus set (in log luminance range from -1 to 1 around the target disk luminance with a unit step size of 0.2 log unit; 11 steps in total) per each of the 30 conditions (6 ring width x 5 background luminance). We then computed the mean of the model cell activities responding to the match disks for each of the 11 luminance-steps, fitted these results with a 5th order polynomial function (i.e. the mean model cell response as a function of match disk luminance). The mean cell response was computed for the target disk of the corresponding condition as well and we searched for the luminance of the match disk that yielded the same mean response as did the target disk.

Comparison of the cell responses between the two original models without any modifications (parasol ganglion cell responses for Wilson's model and photoreceptor responses for van Hateren's model) showed that van Hateren's model readily explained the ring width effect on the brightness of the disk as a function of background luminance difference (Figure 5f), while Wilson's model did not (Figure 5c). Comparably, modifying Wilson's model to include the wide amacrine cell RF produced the ring size effect matching the behavioral data (Figure 5e).

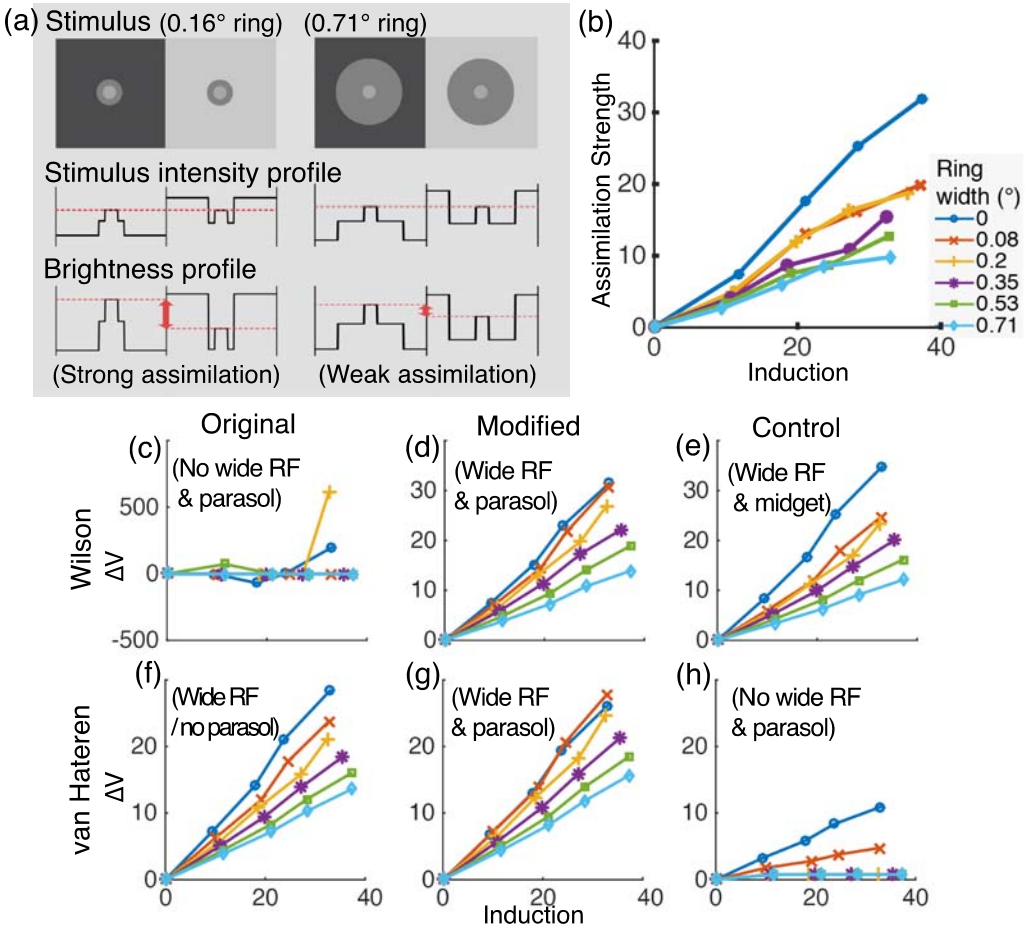

Figure 5. Behavioral and simulation results of Reid and Shapley's experiment (1988). (a) Examples of stimuli with a narrow ring (left) and a wide ring (right). The comparison of stimulus intensity profile with brightness profile schematically illustrates how the narrower induce stronger assimilation compared to the wider ring. (b) The behavioral data on the assimilation strength as a function of difference of the background luminance (labeled 'induction' following the original study by Reid and Shapley) by for different sizes of rings (replotted from Fig 3 in Reid and Shapley, 1988). Larger values indicate stronger assimilation. (c-h) The retinal model simulation results. (c-e) for Wilson's model and (f-h) for van Hateren's model, with the original algorithms (c, f), modified versions (d, g) and control versions (e, h). All are plotted comparably to (b) except that y-axis is ΔV (the luminance of the disk in the lighter background subtracted by the baseline condition, [70, 70] cd/m2 background set, result. The wide RF structure is necessary to predict the stronger assimilation strength for narrower rings comparable to (b).

Eliminating the wide RF component in van Hateren's model removed the systematic ring size effect (Figure 5h). Assimilation was induced only for the two narrowest rings, suggesting that the narrow RFs of interneurons alone cannot explain the systematic ring size effect over the entire ring width range. This result is consistent with an earlier computational study by Heinemann and Chase (1994; see **Discussion**). The synaptic convergence in the parasol pathway was not critical in predicting the overall size dependency in the data pattern in this case (Figure 5d and 5e and Figure 5f and 5g).

Our results demonstrate that the wide RFs of retinal interneurons indeed account for assimilation in Reid and Shapley's data. Moreover, van Hateren's model result implies that this effect could in fact occur at the very first stage of visual processing at the photoreceptor level.

Simulation without Narrow RF

In the previous sections, we compared the model stimulation results when a wide RF was included or not in the model structures and showed that the wide RF was necessary to predict the brightness contrast-to-assimilation data patterns as functions of the decreasing surrounding size in the studies by Helson (1963) and Reid and Shapely (1988). In this section, we show that the wide RF is sufficient to predict most of the surrounding size effect with van Hateren's model (2005; 2007) by simulating the same experiments when the narrow RF component of the horizontal cells was eliminated. We did not perform this simulation with Wilson's model, since the horizontal cells in Wilson's model (1997) have a complex functional structure due to the long-range feedback from the interplexiform layer cells, which governs the light adaptive properties of the entire retinal circuitry, such that it was not possible to remove the horizontal cells or to drastically increase their RF size without an alternative mathematical solution to stabilize the system.

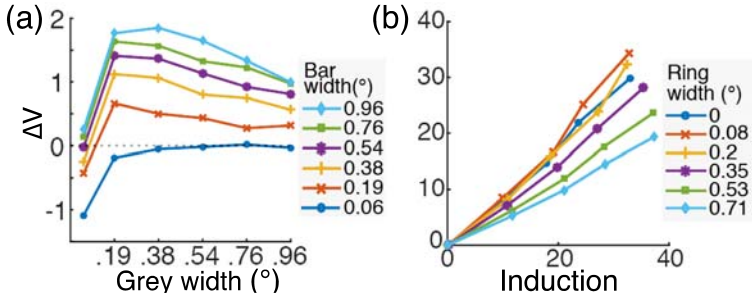

Figure 6. The simulation results of van Hateren's model (2005; 2007) with only the wide RF component of horizontal cells. (a) The result for Helson's experiment (1963). (b) The result for Reid and Shapley's experiment (1988). See and compare with Figure 4g and 5g.

The simulation method and set-up were identical to other simulations except for the removal of the narrow RF component from the horizontal cell RF. The results are plotted in Figure 6. The patterns of the simulation results are comparable to the results in the previous sections (Figure 4g for Helson and Figure 5g for Reid and Shapley), suggesting that the wide RF was mostly responsible for producing the cell responses matching to the contrast-to-assimilation patterns.

Discussion

Simulating the brightness induction experiments with the two biophysical retinal models, we showed that the retinal spatial processing structures explain the effect of the size of the surrounding surface on brightness contrast-to-assimilation phenomena observed by Helson (1963) and Reid and Shapley (1988). The wide RF profile of the retinal feedback interneurons was a critical clue that has been missing for relating the retina to brightness assimilation.

Our approach differs from theoretical modeling of brightness computation. The architectures of the two biophysical models we used are rigorously justified and based on neurophysiological data both anatomically and functionally without any relation to brightness computation. All the spatial processing structures in the original models, including the wide RF profile of horizontal cells in van Hateren's model, were designed to essentially reproduce the spatial response properties of the actual retinal cells. By comparing the effects of these structures on the contrast-to-assimilation phenomena across the two algorithmically-distinct models, we showed that the wide RF robustly explains the effect of surrounding size. We thus conclude that the surrounding-size dependency of the brightness induction phenomena *is very likely to* occur at the retina.

Our results on the local contrast induction are comparable to the earlier computational work by Heinemann and Chase (1994). They proposed a theoretic model of brightness computation in early level visual system and the evaluated model's prediction on Reid and Shapley's experiments (1988). In particular, this model was comprised of three computational steps in which

1) the input stimulus was convolved the stimulus with difference-of-Gaussian (DOG) filter representing the center-surround processing,
2) the output of 1) was thresholded, and
3) the output of 2) was subtracted by its global mean.

The step 3) is based on the notion of Helson's adaptation-theory (Helson, 1938), which proposes that the brightness of a given surface is affected by the average of the luminance elements in the visual field. Such process will allow for long-range surface interaction. Heinemann and Chase reported that the ring width effect in Reid and Shapley's results was mostly explained by 3) in the model because decreasing ring width reduces the contribution of the ring luminance to the global mean. On the other hand, there was no significant difference depending on the ring width in the output of 2), except for the smallest ring width (0.08°; this is comparable to van Hateren's model result without the wide RF in Figure 5h).

However, there are uncertainties regarding the model by Heinemann and Chase (1994). First, it still remains uncertain what kind of neural mechanism generates long-range interaction. If there exists in the visual system a process by which a global mean is computed, what is the neural mechanism of such process? Also, what is the spatial extent of this process? This latter question is important since the relative effect of 3) in brightness computation depends critically on the spatial extent of the mean computation. Heinemann and Chase assumed this to be within 0.5°-1.5° in visual angle at the fovea based on the psychological evidence on the distance of a remote stimulus that influence perception of a foveal stimulus, but if a bigger summation area was assumed, the ring would contribute much less to the mean computation. Our results largely resolve these issues in that the wide RFs of interneurons in the retina can perform the long-range surface interaction of the kind as 3) in Heinemann and Chase's model and that the spatial extent of the wide interneuron RFs provided in neurophysiological studies fit well to the behavioral data.

The long-range surface interaction underlying the size effects in the brightness phenomena can be attributed to the wide RFs of either horizontal cells (as in van Hateren's model) or amacrine cells (as in Wilson's model) in theory. On one hand, various types of wide RF amacrine cells are anatomically identified (Kolb, 1997; Lin & Masland, 2006; MacNeil & Masland, 1998), and it is possible that one of them operates the long-range effect. On the other hand, there is more direct evidence supporting horizontal cells in that a horizontal cell's sensitivity differs between driving stimuli as large as 5° v.s. 10° (Packer & Dacey, 2002; 2005; replicated in van Hateren's model, 2007), as neurophysiologically and computationally shown to result from its wide RF component. Horizontal cells are also argued to contribute to forming most of the ganglion cell RF surround (Lee et al., 2010; McMahon, Packer, & Dacey, 2004), which suggests that the center-surround processing in the retina depends on horizontal cells to a larger degree than amacrine cells. Thus, the long-

range interaction might occur mostly at the very first stage of the visual processing in the photoreceptor-horizontal cell circuit.

Although it is established that the retina regulates spatial-frequency sensitivity of human contrast perception (e.g. see Kelly, 1977; Lee et al., 1990; Shapley & Enroth-Cugell, 1984; Wilson, 1997), brightness induction theories have excluded the retina from discussion in the context of assimilation, assuming that the long-range surface interaction is beyond the spatial scale of any retinal processing (Reid & Shapley, 1988; Rudd, 2010; Heinemann & Chase, 1994). Neither has there been an alternative theory on how the long-range surface interaction occurs, leaving the assimilation phenomena largely unexplained (Fiorentini, 2003; Reid & Shapley, 1988; Rudd, 2010). On the other hand, the current study demonstrates that the spatial scale of the newly discovered wide RF profiles of retinal interneurons fits to the perceptual properties of the long-range surface interaction effect observed in the brightness induction literature (Helson, 1963; Reid & Shapley, 1988). The brightness induction theories may need to be updated accordingly.

As an example, our results provide a new insight on the neural ground of the Retinex theory (Land 1977; Land & McCann, 1971). Retinex theory proposes a general framework in which the lightness of a certain point in a visual scene is well predicted by the mean average of (non-linearly scaled) chain products of luminance ratios along paths that start at arbitrary points all over the scene but always end on the point under consideration. Reid and Shapley (1988) pointed out that their experiments showed that the Retinex formulation should be amended so that far-away regions have less influence than nearby ones, which is something that was independently incorporated into alternative Retinex implementations (Provenzi, Fierro, Rizzi, De Carli, Gadia & Marini, 2007; Bertalmío, Caselles, & Provenzi, 2009) and related perceptually based algorithms (Rizzi, Gatta and Marini, 2003). The current study proposes that precisely this kind of weighted summation process can be accomplished by wide-RF interneuron feedback. Since there are also works suggesting a connection between Retinex and neuroscience (Bertalmío et al., 2009; Bertalmío & Cowan, 2009; Bertalmío, 2014a; 2014b), at present we are working at establishing what kind of relationship there is between those models and the ones employed in this study.

Edge-integration theory (Rudd, 2010; 2013; Rudd & Zemach, 2004; 2007) is also based on the Retinex framework and shows that the ring size effect on brightness induction in the disk-and-ring stimuli can be well predicted by a weighted sum of the log-luminance ratios of the disk and the ring and of the ring and the background, a result which again can be achieved through wide-RF interneuron feedback.

The interneuron feedback mechanism in retinal processing is also closely related to chromatic induction since horizontal / amacrine cells generate color opponency in the midget retinal pathway (Crook, Manookin, Packer, & Dacey, 2011; Dacey, 1996; 1998; 2000; Lebedev & Marshak, 2007; Lee et al., 2011). In a chromatic version of Helson's experiment (Fach & Sharpe, 1986), the spatial scale of color bars that induced hue assimilation was comparable to the bar width that induced brightness assimilation in Helson's experiment. However, further increasing the bar width did not enhance hue contrast any further, unlike the systematic brightness contrast increment at the corresponding bar width range in Helson's result (for spatial properties of the chromatic assimilation, see also Moulden, Kingdom, & Wink, 1993; Smith, Jin, & Pokorny, 2001; Zaidi, Yoshimi, Flanigan, & Canova, 1992). Noticing that it is at this wider bar range that wide interneuron RFs are necessary to account for brightness induction phenomena in our results, the wide interneuron RF may not have a significant effect on color processing in the midget pathway and this issue requires further assessment.

The wide RF in our simulations produced assimilation as in the *mechanical* definition, i.e. a long-range surface interaction mechanism by which the brightness of the target area is pulled toward the surrounding (bars or rings) luminance *against the local contrast between the target and the surrounding*, as fundamentally assumed in Reid and Shapley's study (1988) (note, assimilation measurement in Reid and Shapley's experiment was implicit). However, we are hesitant to argue that this mechanical definition is reciprocal to *perceivable* assimilation (i.e. the target brightness is pulled toward the surrounding luminance *compared to the target's physical luminance*). The simulation of Helson's experiment (1963) showed that *perceivable* assimilation (the narrowest bar) required spatial convergence in the parasol pathway, whereas the long-range interaction by wide RF was sufficient but not necessary. *Perceivable* assimilation is further shown to involve post-retinal mechanisms including orientation/depth processing and attention (e.g. Blakeslee & McCourt, 2004; Festinger, Coren, & Rivers, 1970; Kingdom, 2011; Rudd, 2010; Shevell, Holliday, & Whittle, 1992; Sugita, 1994). Indeed, the output signals from the retina are subject to more complex information processing in the cortex and brightness computation must result from this whole range of processing. Meanwhile, our results show that the retina is a significant starting point of brightness assimilation and operates long-range surface interaction.

Conclusion

We investigated the neural basis of surrounding-size-dependency of contrast-to-assimilation phenomena demonstrated in the behavioral studies of Helson (1963) and Reid

and Shapley (1988) by simulating the experiments in two existing biophysical retinal models (van Hateren, 2005; 2007; Wilson, 1997). With the proper modifications, both of the models generated the responses that match to the pattern of the behavioral data. The wide RF structure of retinal interneurons was critical in predicting the surrounding size effect in both of the experiments. While the contribution of this wide RF component to the interneuron RF formation in the models was much smaller than the narrow RF contribution (Figure 3), our results show that this subtle addition of the wide RF component enables the long-range surface interaction and predicts the assimilation phenomena, at least in the sense that Reid and Shapley (1988) defined it. We conclude that retinal processing bears importance in brightness assimilation unlike what has been previously assumed.

Acknowledgement

This work was supported by the European Research Council, Starting Grant ref. 306337, by the Spanish government, grant ref. TIN2012-38112, and by the Icrea Academia Award.

References

Arend, L. E., Buehler, J. N., and Lockhead, G. R. (1971). Difference information in brightness perception. *Perception & Psychophysics, 9*, 367-379.

Benardete, E. A., and Kaplan, E. (1999a). The dynamics of primate M retinal ganglion cells. *Visual Neuroscience, 16*, 355-368.

Benardete, E. A., and Kaplan, E. (1999b). Dynamics of primate P retinal ganglion cells: Responses to chromatic and achromatic stimuli. *Journal of Physiology. 519*, 775-790.

Bertalmío, M. (2014a). From image processing to computational neuroscience: a neural model based on histogram equalization. *Frontiers of Computational Neuroscience, 8*, 1-9.

Bertalmío, M. (2014b). *Image Processing for Cinema.* Boca Raton, FL: CRC Press.

Bertalmío, M., Caselles, V., and Provenzi. E. (2009). Issues about retinex theory and contrast enhancement. *International Journal of Computer Vision, 83*, 101–119.

Bertalmío, M., and Cowan, J. (2009). Implementing the Retinex algorithm with Wilson-Cowan equations. *Journal of Physiology - Paris, 103*, 69-72.

Blakeslee, B., and McCourt, M. E. (2004). A unified theory of brightness contrast and assimilation incorporating oriented multiscale spatial filtering and contrast normalization. *Vision Research, 44*, 2483-2503.

Campbell, F. W., and Gubisch, R. W. (1966). Optical quality of the human eye. *Journal of Physiology, 186*, 558-578.

Crook, J. D., Manookin, M. B., Packer, O. S., and Dacey, D. M. (2011). Horizontal cell feedback without cone type-selective inhibition mediates "red–green" color opponency in midget ganglion cells of the primate retina. *Journal of Neuroscience, 31*, 1762- 1772.

Dacey, D. M. (1996). Circuitry for color coding in the primate retina. *Proceedings of National Academy of Science USA, 93*, 582-588.

Dacey, D. M. (1998). Primate retina: cell types, circuits and color opponency. *Progress in Retinal and Eye Research, 18*, 737-763.

Dacey, D. M. (2000). Parallel pathways for spectral coding in primate retina. *Annual Review of Neuroscience, 23*, 743-775.

Fach, C., and Sharpe, L. T. (1986). Assimilative hue shifts in color gratings depend on bar width. *Perception & Psychophysics, 40*, 412-418.

Festinger, L., Coren, S., and Rivers, G. (1970). The effect of attention on brightness contrast and assimilation. *The American Journal of Psychology, 83*, 189-207.

Fiorentini, A. (2003). Brightness and lightness. In L. M. Chalupa & J. S. Werner (Eds.), *The Visual Neuroscience, Vol. 2* (pp. 881–891), Cambridge, MA: MIT Press.

Fry, G. A. and Alpern, M. (1953). Effect of a peripheral glare source upon the apparent brightness of an object. *Journal of Optical Society of America, 43*, 189-195.

Heinemann, E. G., and Chase, S. (1994). A quantitative model for simultaneous brightness induction. *Vision Research, 35*, 2007-2020.

Helson, H. (1938). Fundamental problems in color vision. 1. The principle governing changes in hue, saturation, and lightness of non-selective samples in chromatic illumination. *Journal of Experimental Psychology, 23*, 439-476.

Helson, H. (1963). Studies of anomalous contrast and assimilation. *Journal of Optical Society of America, 53*, 179-184.

Hennig, M. H., Funke, K., and Wörgötter, F. (2002). The influence of different retinal sub-circuits on the non-linearity of ganglion cells behavior. *Journal of Neuroscience, 22*, 8726-8738.

Kaplan, E., and Benardete, E. (2001). The dynamics of primate retinal ganglion cells. *Progress in Brain Research, 134*, 17-34.

Kelly, D. H. (1977). Visual contrast sensitivity. *Optica Acta: International Journal of Optics, 24*, 107-129.

Kingdom, F. A. A. (2011). Lightness, brightness and transparency: A quarter century of new ideas, captivating demonstrations and unrelenting controversy. *Vision Research, 51*, 652-673.

738 Kolb, H. (1997). Amacrine cells of the mammalian retina: Neurocircuitry and functional
739 roles. *Eye, 11*, 904-923.
740 Land, E. H. (1977). The Retinex theory of color vision. *Scientific American, 237*, 108-128.
741 Land, E. H., and McCann, J. J. (1971). Lightness and retinex theory. *Journal of Optical*
742 *Society of America, 61*, 1-11.
743 Lebedev, D. S., and Marshak, D. W. (2007). Amacrine cell contributions to red-green color
744 opponency in central primate retina: A model study. *Visual Neuroscience, 24*, 535-547.
745 Lee, B. B., Martin, P. R., and Grünert, U. (2010). Retinal connectivity and primate vision.
746 *Progress in Retinal and Eye Research, 29*, 622-639.
747 Lee, B. B., Pokorny, J., Smith, V. C., Martin, P. R., and Valberg, A. (1990). Luminance and
748 chromatic modulation sensitivity of macaque ganglion cells and human observers.
749 *Journal of Optical Society of America A, 7*, 2223-2236.
750 Lee, B. B., Sun, H., and Valberg, A. (2011). Segregation of chromatic and luminance signals
751 using a novel grating stimulus. *Journal of Physiology, 11*, 59-73.
752 Lin, B., and Masland, R. H. (2006). Populations of wide-field amacrine cells in the mouse
753 retina. *The Journal of Comparative Neurology, 499*, 797-809.
754 MacNeil, M. A., and Masland, R. H. (1998). Extreme diversity among amacrine cells:
755 Implications for function. *Neuron, 20*, 971-982.
756 McMahon, M. J., Packer, O. S., and Dacey, D. M. (2004). The classical receptive field
757 surround of primate parasol ganglion cells is mediated primarily by a non-GABAergic
758 pathway. *Journal of Neuroscience, 24*, 3736-3745.
759 Moulden, B., Kingdom, F., and Wink, B. (1993). Colour pools, brightness pools,
760 assimilation, and the spatial resolving power of the human colour-vision system.
761 *Perception, 22*, 343-351.
762 Packer, O. S., and Dacey, D. M. (2002). Receptive field structure of H1 horizontal cells in
763 macaque monkey retina. *Journal of Vision, 2*, 272-292.
764 Packer, O. S., and Dacey, D. M. (2005). Synergistic center-surround receptive field model of
765 monkey H1 horizontal cells. *Journal of Vision, 5*, 1038-1054.
766 Passaglia, C. L., Enroth-Cugell, C., and Troy, J. B. J. (2001). Effects of remote stimulation on
767 the mean firing rate of cat retinal ganglion cells. *Journal of Neuroscience, 21*, 5794–
768 5803.
769 Perlman, I., and Normann, R. A. (1998). Light adaptation and sensitivity controlling
770 mechanisms in vertebrate photoreceptors. *Progress in Retinal Eye Research, 17*, 523-
771 563.

Provenzi, E., Fierro, M., Rizzi, A., De Carli, L., Gadia, D., and Marini. D. (2005). Random spray Retinex: A new Retinex implementation to investigate the local properties of the model. *IEEE Transactions on Image Processing, 16*, 162-171.

Ratliff, F. (1971). Contour and contrast. *Proceedings of American Philosophical Society, 115*, 150-163.

Reid, C. R., and Shapley, R. (1988). Brightness induction by local contrast and the spatial dependence of assimilation. *Vision Research, 28*, 115-132.

Rudd, M. E. (2010). How attention and contrast gain control interact to regulate lightness contrast and assimilation: A computational neural model. *Journal of Vision, 10*, 1-37.

Rudd, M. E. (2013). Edge integration in achromatic color perception and the lightness–darkness asymmetry. *Journal of Vision, 13*, 1-30.

Rudd, M. E., and Zemach, I. K. (2004). Quantitative properties of achromatic color induction: An edge integration analysis, *Vision Research, 44*, 971-981.

Rudd, M. E., and Zemach, I. K. (2007). Contrast polarity and edge integration in achromatic color perception. *Journal of Optical Society of America A, 24*, 2134-2156.

Shah, S., and Levine, M. D. (1996). Visual information processing in primate cone pathways – Part I: A model. *IEEE Transactions on Systems, Man, and Cybernetics Part B: Cybernetics, 26*, 259-274.

Shapley, R., and Enroth-Cugell, C. (1984). Visual adaptation and retinal gain-controls. *Progress in Retinal and Eye Research, 3*, 263-346.

Shapley, R., and Reid, R. C. (1985). Contrast and assimilation in the perception of brightness. *Proceedings of National Academy of Science USA, 82*, 5983-5986.

Shevell, S. K., Holliday, I., and Whittle, P. (1992). Two separate neural mechanisms of brightness induction. *Vision Research, 32*, 2331-2340.

Smith, V. C., Jin, P.Q., and Pokorny, J. (2001). The role of spatial frequency in color induction. *Vision Research, 41*, 1007-1021.

Solomon, S. G., Lee, B. B., and Sun, H. (2006). Suppressive surrounds and contrast gain in magnocellular-pathway retinal ganglion cells of macaque. *Journal of Neuroscience, 26*, 8715-8726.

Sugita, Y. (1994). Contrast and assimilation on different depth planes. *Vision Research, 35*, 881-884.

Thoreson, W. B., and Mangel, S. C. (2012). Lateral interactions in the outer retina. *Progress in Retinal and Eye Research, 31*, 407-441.

van Hateren, H. (2005). A cellular and molecular model of response kinetics and adaptation in primate cones and horizontal cells. *Journal of Vision, 5*, 331-347.

van Hateren, J. H. (2007). A model of spatiotemporal signal processing by primate cones and horizontal cells. *Journal of Vision, 7*, 1-19.

van Hateren, J. H. (2008). Fast recursive filters for simulating nonlinear dynamic systems. *Neural Computation, 20*, 1821-1846.

van Hateren, J. H., and Lamb, T. D. (2006). The photocurrent response of human cones is fast and monophasic. *BMC Neuroscience, 7*, 1-8.

Watson, A. B., and Yellott, J. I. (2012). A unified formula for light-adapted pupil size. *Journal of Vision, 12*, 10-16.

Wilson, H. R. (1997). A neural model of foveal light adaptation and afterimage formation. *Visual Neuroscience, 14*, 403-423.

Wohrer, A., and Kornprobst, P. (2009). Virtual retina: A biological retina model and simulator, with contrast gain control. *Journal of Computational Neuroscience, 26*, 219-249.

Zaidi, Q., Yoshimi, B., Flanigan, N., and Canova, A. (1992). Lateral interaction within color mechanisms in simultaneous induced contrast. *Vision Research, 32*, 1695-1707.